Jurnal Teknologi

Full paper

Hydrodynamic Resistance analysis of New Hull Design for Multipurpose Amphibious Vehicle Applying with Finite Volume Method

M. Nakisa[a,c], A. Maimun[b*], Yasser M. Ahmed[a,d], F. Behrouzi[a], S. Steen[e], A. Tarmizi[a]

[a]*Faculty of Mechanical Engineering, Universiti Teknologi Malaysia, 81310 UTM Johor Bahru, Johor, Malaysia*
[b]*Marine Technology Center, Universiti Teknologi Malaysia, 81310 UTM Johor Bahru, Johor, Malaysia*
[c]*Faculty of Engineering, Islamic Azad University, Boushehr Branch, Boushehr, Iran*
[d]*Faculty of Engineering, Alexandria University, Alexandria, Egypt*
[e]*Rolls-Royce University Technology Centre , Norwegian University of Science and Technology, N-7491 Trondheim, Norway*

*Corresponding author: adi@fkm.utm.my

Article history

Received :25 December 2014
Received in revised form :
25 March 2015
Accepted :15 May 2015

Graphical abstract

Multipurpose Amphibious Vehicle

Abstract

This paper numerically investigated the hydrodynamic resistance of Multipurpose Amphibious Vehicles (MAV) in three bow shapes to approach the better hull bow shape design. This type of vehicle and other blunt-shaped floating vehicles encounter the problem of a large bow wave forming at high speeds. This wave formation is accompanied by higher resistance and at a critical speed results in bow submergence or swamping. Three new shapes of hull bow design for the multipurpose amphibious vehicle were conducted at several speeds to investigate the hydrodynamic phenomena using Computational Fluid Dynamics (CFD, RANS code) which is applied by Ansys-CFX14.0 and Maxsurf. The vehicle's hydrodynamic bow shapes were able to break up induced waves and avoid swamping. Comparative results with the vehicle fitted with U-shape, V-shape and Flat-shape of hull bow, showed that the U-shape of the hull bow has reduced the total resistance to 20.3% and 13.6% compared with the V-shape and flat shape respectively. Though, the U-shape of hull bow is capable to increase the amphibious operating life and speed of vehicle in calm water. Also it has ability to reduce the vehicle's required power, fossil fuel consumption and wetted hull surface.

Keywords: Multipurpose amphibious vehicle; hydrodynamic resistance; RANS code

1.0 INTRODUCTION

The development of landing craft and amphibious vehicles has a long history beginning in WWII with the Higgins LCVP[1] extending to the 35 kt hydrofoil, LVH[2], and the 70 kt aircushion LCAC used today[3]. Included in this group are the M59 Amphibious Personnel Carrier and the air-transportable M113 Amphibious Personal Carrier introduced in 1960. By 2000, Over 76,000 M113 variants were built[4]. The M113 is a tracked vehicle powered by an eight-cylinder 215 hp engine. In the amphibious operation, the M113 operates at 5.8 km/h (3.13 kt), and on land, it reaches speeds of 64 km/h. It steers on land and water by changing the speed of either track. Designed for air transport, the M113 is compact and lightweight. It has weight saving aluminium armour plate. The M113 dimensions are 4.86 m long, 2.686 m wide and 1.85 m high. At its weight of 11,253 kg, it has an amphibious draft of 1.3 m. The box-shaped hull results in a length to beam ratio L/B51.80 and a beam to draft ratio B/T52.12. A study of new hull design of Multipurpose Amphibious Vehicles (MAV) was conducted to enhance its amphibious capability by considering floatability, stability and resistance/propulsion characteristics. Initial resistance and flow visualization simulation showed that water enters into the driver compartment and that there is a need for a hydrodynamic bow shape in order to prevent water build-up at the front of the driver's place[5].

Traditionally, ships have been optimized for minimum fuel consumption in calm water. For amphibious vehicles, this has led to very blunt bow shapes. Such bow shapes have high added resistance due to waves. Thus, one might think that the optimum bow shape, when realistic wave conditions are taken into account, should be more slender or hydrodynamic shapes than the current one. Furthermore, the operational area of the ship (the route it sails) could influence what is the optimum bow shape.

Amphibious vehicles such as amphibious assault vehicles and amphibious armoured personnel carriers have been utilized in the military services for many years[6]. Their mission specifications included the amphibious operations described as to be deployed from a ship in calm to moderate seas and to reach the shore at a reasonable time. They are usually powered by two water-jets at a maximum water-borne speed of about 13 km/h. On the other hand most of these amphibious vehicles are designed for land operations only and their operations in water are limited to

passing through rivers safely at a specified speed without satisfying floatation requirements. Therefore, the floatability and stability requirements of these vehicles are optional features required only for deep river operations.

In the open literature, there are only a few published papers on the design principles of amphibious vehicles. It is investigated several waterjet systems for Marine Corps applications[7]. A flush type waterjet propulsion unit applied for a Multipurpose Amphibious Vehicles (MAV) that can cross rivers and lakes at a speed of 10 km/h with a twin waterjet propulsion system. Self-propulsion tests were carried out by using a 1/5 scale Amphibious model to estimate the required effective power. ITTC 96 momentum flux method was utilized to evaluate the performance of the system. The main parameter on the powering requirement of the MAV is the impeller size, an increase of 35% in the waterjet impeller diameter may result in a 38% power reduction, or a 13% increase in the vehicle speed may be achieved for the MAV tested[8].

■2.0 MODELING AND GOVERNING EQUATIONS

The MAV is equipped with watertight compartments to achieve floatation capability. The vehicle is also equipped with additional water pumps in order to pump out the uncontrolled water ingress during the river crossing mission. Three geometry designs of MAV are shown in Figures 1-3. The Characteristics of Multipurpose Amphibious Vehicle are given in Table 1. Appendages, which are not a part of the main body such as wheels, drive trains etc. are considered as watertight compartments and added separately in stability calculations. In addition to floatability, the vehicle should also be stable in a floating condition.

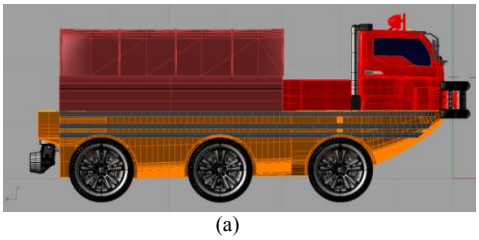

(a)

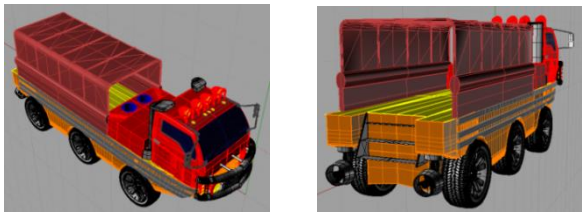

(b)

Figure 1 (a) Side view (b) Prespective view of multipurpose amphibious vehicles

Figure 4 and Table 2 show the computational domain and mesh elements which is modeled and simulated in analysis-CFX 14.0 using Finite Volume Method (FVM).

Table 1 Characteristics of multipurpose amphibious vehicle

Loading Condition	Actual size	Model Size	Unit
L_{WL}	6.607	1.65175	m
Beam	2.024	0.506	m
Draft	0.99	0.2475	m
Displaced volume	5.314	0.08303	m^3
Wetted area	31.719	0.33212	m^2
Prismatic coeff.	0.559	0.559	------
Waterplane area coeff.	0.665	0.665	------
LCG from midships	2.726	0.6815	m
Transom draft	0.025	0.00625	m
Max sectional area	1.438	0.08987	m^2
Deadrise at 50% LWL	19.33	19.33	deg.
Hard chine or Round bilge	Round bilge	Round bilge	------
Headwind	0	0	kts
Scale	1	4	------
Air density	0.001	0.001	tonne/m^3
Kinematic viscosity	1.1883E-06	1.1883 E-06	m^2/s
Water Density	1.025	1.00	tonne/m^3

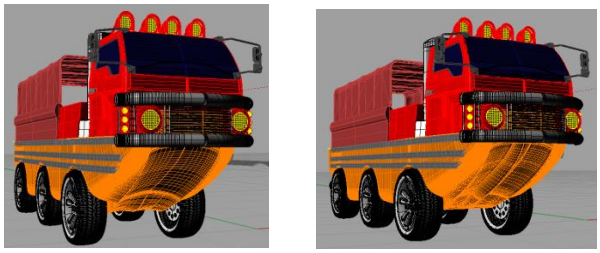

(a) (b)

Figure 2 (a) U bow shape hull, (b) V bow shape hull

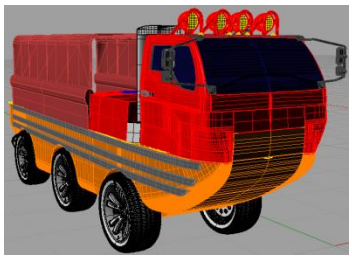

Figure 3 Flat bow shape hull

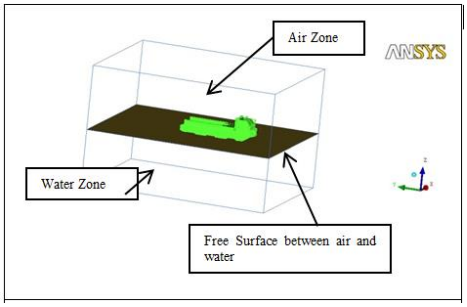

Figure 4 Multipurpose amphibious vehicle computational domain

Table 2 Mesh elements number

Total Elements	Total Nodes
904287	158448

The shear stress transport (SST) turbulence model had been used in this study, because it gave the best results in comparison with other turbulence models. The equations are shown as follows:

Equation of κ:

$$\frac{\partial}{\partial t}(\rho k)+\frac{\partial}{\partial x_i}(\rho k u_i)=\frac{\partial}{\partial x_j}\left(\Gamma_k\frac{\partial k}{\partial x_j}\right)+G_k-Y_k+S_k \quad (4)$$

Equation of ω:

$$\frac{\partial}{\partial t}(\rho\omega)+\frac{\partial}{\partial x_i}(\rho\omega u_i)=\frac{\partial}{\partial x_j}\left(\Gamma_\omega\frac{\partial \omega}{\partial x_j}\right)+G_\omega-Y_\omega+D_\omega+S_\omega \quad (5)$$

Where G_κ and $G_\omega$express the generation of turbulence kinetic energy due to mean velocity gradients and ω. Γ_κ and Γ_ω express the active diffusivity of κ and ω. Y_κ and Y_ω represent the dissipation of κ and ω due to turbulence. D_ω expresses the cross-diffusion term, S_κ and S_ω are user-defined source terms[9,10].

The forces and moments acting on the hull can be approximated by the following polynomials of v′ and r′ by the following expressions[11].

$$X_H=\frac{1}{2}\rho L^2U^2[X'_{\dot{u}}\dot{u}'+X'_{vr}v'r'+X'_{vv}v'^2+X'_{rr}r'^2]+\frac{1}{2}\rho L^2U^2R'_{TM} \quad (6)$$

$$Y_H=\frac{1}{2}\rho L^2U^2[Y'_{\dot{v}}\dot{v}'+Y'_{\dot{r}}\dot{r}'+Y'_vv'+Y'_{vvv}v^3+Y'_{vvr}v'^2r'+Y'_{vrr}v'r'^2+Y'_{rrr}r'^3] \quad (7)$$

$$N_H=\frac{1}{2}\rho L^3U^2[N'_{\dot{v}}\dot{v}+N'_{\dot{r}}\dot{r}'+N'_vv'+N'_rr'+N'_{vvv}v^3+N'_{vvr}v'^2r'+N'_{vrr}v'r'^2+N'_{rrr}r'^3] \quad (8)$$

The primes in Equation 6, Equation7 and Equation 8 refer to the non-dimensional quantities, defined as the following:

$$v'=\frac{v}{U};\quad \dot{v}'=\frac{\dot{v}L}{U^2};\quad r'=\frac{rL}{U};\quad \dot{r}'=\frac{\dot{r}L^2}{U^2} \quad (9)$$

$$X'=\frac{X}{\frac{\rho}{2}L^2U^2};\quad Y'=\frac{Y}{\frac{\rho}{2}L^2U^2};\quad N'=\frac{N}{\frac{\rho}{2}L^3U^2} \quad (10)$$

$$R'=\frac{R}{\frac{\rho}{2}L^2U} \quad (11)$$

R = Ship Resistance

N is sum of yaw moments acting on the MAV and N'_v , $N'_r, N'_{vv}, N'_{rr}, N'_{vvr}, N'_{vrr}, N'_{rrr}$ are hydrodynamic coefficients for the yaw moment, also Y is sum of forces acting on the ship in the transverse direction and Y'_v , $Y'_r, Y'_{vv}, Y'_{rr}, Y'_{vvr}, Y'_{vrr}, Y'_{rrr}$ are hydrodynamic coefficients for sway force. X is sum of forces acting on the MAV in the longitudinal direction[12,13].

The computational setting for using the ANSYS-CFX is tabulated in Table 3 as follows:

Table 3 Computational setting

Parameter	Setting
Computing	64-bit Desktop pc 16GB of RAM
Simulation type	Steady state
Mesh type	Unstructured hybrid(tetrahedral/prism)
Turbulence model	k-w (Shear stress transport)
Wall modelling Automatic	wall function based on a law of the wall formulation
Advection scheme	CFX high resolution

■3.0 RESULTS AND DISCUSSION

Total calm water resistance against Froude number are shown in Figure 5. Considering to following resistance graphs, U-shape of hull bow has lowest resistance in service speed which is 12 kt because in these high speeds the induced waters and waves are guided to go underneath of the U-shape of hull bow and both sides of hull. Wave fraction resistance in V-shape of hull bow has more significant effect for increasing the total resistance. In addition, this phenomena cause to increase the frictional resistance, added resistance and pressure resistance. Total resistance almost are same in lower than 7 kt for all bow shapes because the pressure resistance and frictional resistance and wetted surface in low speed are same in U-shape, V-shape and Flat-shape hull bow designs.

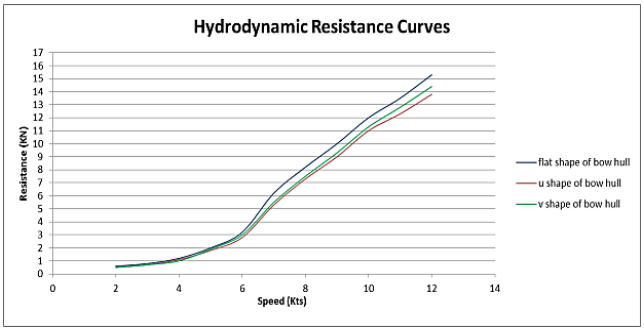

Figure 5 Scheme of computational domain

The resistance curves plotted against Froude number gives the optimum design for the U-shape of hull bow design in speeds more than 10 kt, because in these range of speeds, the Multipurpose Amphibious Vehicle takes up and consequently the wetted surface and friction resistance decreases. Fuel consumption reduction and speed increasing are related to total resistance in service speed range as well.

The ratios of pressure and frictional resistance respect to total resistance are approximately 25% and 75%, respectively, up to Fn=0.4, but they become 50% and 50%, respectively, at the highest Fn as a result of the increase of pressure component, which is most likely attributable to large deformation of free surface in the vicinity of the MAV hull. The Flat-shape of hull bow and V-shape of hull bow design have more frictional and pressure resistance than U-shape one. Total resistance of U-shape of hull bow is 20.3% and 13.6% lower than V-shape and Flat-shape of hull bow designs, respectively, in service speed range.

■4.0 CONCLUSION

The article has investigated the performance of the three different shapes designed of bow hull and optmized the best performance in accordance of the total resistance during the operating of the Multipurpose Amphibious Vehicle in various speed ranges. However, the added resistance is mainly dependent on the shape of the hull bow of designed vehicle.

When the U-shape of hull bow of MAV faced the water and wave, it forced the vehicle to flow up, which resulted to reduce the draft of the water and wave resistance, in addition, the wetted hull, friction resistance, pressure resistance, power of the vehicle, fossil fuel consumption and wave breaking resistance of the U-shape hull bow decreased compared with the others bow shapes. Meanwhile, the U-shape of the hull bow has reduced the total resistance to 20.3% and 13.6% compared with the V-shape and flat shape respectively. Though out, the U-shape of the hull bow is capable to increase the amphibious operating life and speed of vehicle.

Acknowledgements

The authors would like to express their sincere gratitude to Universiti Teknologi Malaysia (UTM) for financial support given to this research work.

References

[1] G. Haddock and R. Latorre. 1995. A Look Back on 1942 Combat and Production, An Example of Successful Employee Empowerment at Higgins Industries. *Journal of Ship Production*. 11(3): 159–170.
[2] D. Carl. June 1965. New Amphibious Vehicle Progress Part 3nlanding Craft, Assault LCA and Landing Vehicle Hydrofoil (LVH). Naval *Engineering Journal*. 77(3): 18–25.
[3] R. Alexander and R. M. Alexander. 1963. Design of Landing Craft for Marine Corps Action. *Naval Engineering Journal*. 75(1): 163–170.
[4] C. Foss. 2003. *Jane's Tank and Combat Vehicle Recognition Guide.* Harper Collins, New York.
[5] S. Helvacioglu, I. H. Helvacioglu and B. Tuncer. 2011. Improving the River Crossing Capability of an Amphibious Vehicle. *Ocean Engineering*. 38: 2201–2207.
[6] K. Jaswar , Siow, C.L., Maimun, A., Guedes Soares. 2014. Estimation of Electrical-wave Power in Merang Shore, Terengganu, Malaysia. *Jurnal Teknologi (Sciences and Engineering).* 66(2): 9–14.
[7] Marine Corps Warfighting Publication. 2005. Employment of Amphibious Assault Vehicles (AAVs), /http://www.doctrine.usmc.mils, MCWP. 3–13.
[8] J. G. Sticker, A. J. Becnel and J. G. Purnell. 1994. Advanced Waterjet Systems. *Nav. Eng. J.* 106(5): 100–109.
[9] H. H. Chun, B. H. Ahn and S. M. Cha. 2003. Self-Propulsion Test and Analysis of an Amphibious Tracked Vehicle with Waterjet. In: Proceeding of World Maritime Technology Conference and SNAME Annual Meeting, Paper No. D6 (D-133), USA.
[10] M. Nakisa, Malik, A. M. A , Ahmed, Y. M. , Steen, S., Behrouzi, F., Hassanzadeh, R., Sabki, A. F. 2014. Propeller Effect on 3D Flow at the Stern Hull of a LNG Carrier Using Finite Volume Method. *Applied Mechanics and Materials.* 554: 566–570.
[11] M. Nakisa, A. Maimun, A. Y. Sian, Yasser M. Ahmed, A. Priyanto, Jaswar, F. Behrouzi. 2013. Three-dimensional Numerical Analysis of Restricted Water Effects on the Flow Pattern Around Hull and Propeller Plane of LNG Ship. *International Journal of Mechanics*. 7(3): 234–241.
[12] L. Larsson and H. C Raven. 2010. Principles of Naval Architecture Series-Ship Resistance and Flow. Society of Naval Architects and Marine Engineers (SNAME).
[13] K. MINSAAS and S. STEEN. 2008. Lecture Notes-Ship Resistance, Department of Marine Technology–NTNU, Leishman J. Dynamic stall experiments on the NACA 23012 aerofoil. *Experiments in Fluids*. 9(1): 49e58.